Measuring the Transient Extensional Rheology of Polyethylene Melts Using the SER Universal Testing Platform

Martin Sentmanat
Senkhar Technologies, LLC
Akron, OH

Benjamin N. Wang,
Institute for Soldier Nanotechnology and Department of Chemical Engineering
Massachusetts Institute of Technology
Cambridge, MA 02139

Gareth H. McKinley
Hatsopoulos Microfluids Laboratory and Institute for Soldier Nanotechnology
Department of Mechanical Engineering
Massachusetts Institute of Technology
Cambridge, MA 02139

SYNOPSIS

We use a new extensional rheology test fixture that has been developed for conventional torsional rheometers to measure the transient extensional stress growth in a number of different molten polyethylene samples including a linear low density polyethylene (Dow Affinity PL 1880), a low density polyethylene (Lupolen 1840H) and an ultrahigh molecular weight polyethylene (UHMWPE). The transient uniaxial extensional viscosity functions for the LLDPE and LDPE samples have both been reported previously in the literature using well-established instruments and this allows us to benchmark the performance of the new test fixture. Transient stress growth experiments are carried out over a range of Hencky strain rates from 0.003 s^{-1} to 30 s^{-1} and the data shows excellent agreement with the published material functions. At deformation rates greater than 0.3 s^{-1} a true steady state extensional viscosity is not obtained in the LDPE samples due to the onset of necking failure in the elongating strips of polymer; however the limiting values of the transient extensional viscosity at the onset of sample failure agree well with previously published values for the steady state extensional viscosity. This apparent steady-state extensional viscosity first increases with deformation rate before ultimately decreasing as approximately $\dot{\varepsilon}^{-0.5}$. In addition we perform extensional step-strain measurements at small Hencky strains and demonstrate good agreement with the relaxation modulus obtained from shear rheometry. Extensional creep measurements are performed over a range of constant imposed tensile stresses and also agree well with the measured shear creep compliance. Finally, tensile stress relaxation experiments are carried out after a range of imposed Hencky strains. These tests demonstrate that following large extensional deformations the tensile stresses relax nonlinearly and also that, beyond a critical strain, the material is unstable to viscoelastic necking and rupture. Additional transient extensional stress growth measurements using highly entangled linear UHMWPE samples show greatly reduced strains to failure, that are in agreement with the predictions of the Considère theory.

KEYWORDS: Extensional rheology, strain-hardening, tensile creep, polyethylene, necking failure.

I. Introduction

Measurement of the transient uniaxial extensional viscosity for a polymeric material remains a technical challenge. The situation has been somewhat alleviated in recent years by the development of commercial instrument designs such as the RME [Meissner & Hostettler, 1994]; however, even when a single common instrument is available, careful documentation and control of the test protocols and sample preparation is essential to avoid systematic deviations in results obtained using a single polymeric sample [Schulze et al. 2001]. Many of these experimental difficulties are described in an early review article [Meissner, 1985] and in the work of Schweizer [Schweizer 2000].

A recurring theme and important feature of the advances in extensional rheometry over the past thirty years has been the emphasis on well-controlled, widely-distributed test materials and round-robin inter-laboratory comparisons of different instrumental techniques and operating conditions. This was a hallmark of the early work on the IUPAC-A low density polyethylene by Laun, Münstedt and Meissner using stress-controlled and rate-controlled instruments of widely differing design [Laun & Münstedt, 1979]. This IUPAC material became an international standard reference material which could be used to validate the dynamical response of new rheometer designs and to which other materials could then be compared [Münstedt & Laun 1979; 1981].

Early attempts at repeating this success in extensional rheometry of polymer solutions using the polyisobutylene-based M1 test fluid [Sridhar 1990] were met with disappointment [James & Walters, 1993]. However, the wide scatter in these measurements arose because of the strong strain-rate and strain sensitivity of the extensional stresses exhibited in polymer solutions and the widely-disparate design of the instruments which resulted in non-homogeneous kinematics. More recent inter-laboratory comparisons using a series of well-characterized dilute polystyrene solutions and a common design of filament stretching rheometer, have shown very good agreement [Anna et al. 2001]. The test instruments that were involved in this study were of similar overall design to the original Münstedt Tensile Rheometer [Münstedt, 1979]; however, because of the increased importance of gravity, surface tension and inertia, special design considerations must be incorporated [McKinley & Sridhar, 2002].

In the present work we seek to evaluate the performance of a new test fixture, known as the SER, developed for elongational rheometry by Sentmanat [2003a, b]. The instrument employs the fiber windup technique first described by Macosko and Lorntson [1973] in which a rotating fixture is mounted on the transducer of a conventional torsional rheometer. Further analysis of the kinematics and enhancements to this basic configuration were described by Connelly & coworkers [Connelly et al. 1979; Pearson & Connelly, 1982] and by Padmanabhan

et al. [1996]. However a limitation encountered in all of these previous studies was the onset of non-uniform stretching at moderate strains due to the no-slip boundary condition acting at the rigid (non-rotating) clamped end of the sample. In the SER fixture, this problem is circumvented by the use of a pair of counter-rotating rollers. Extensive experimental details of the instrument design and its dynamical range are provided in a recent publication [Sentmanat, 2004]; however, measurements from the instrument have not, until now, been benchmarked against existing data for a standard viscoelastic reference material. The original IUPAC A material is no longer a viable benchmark material due to irreversible aging over the past 30 years [Laun, 2003]. However, another low density polyethylene (BASF Lupolen 1840H) has recently been shown to exhibit a very similar response in extensional flow [Münstedt et al. 1998]. A closely-related grade (Lupolen 1810H) containing an anti-oxidant stabilizer package and possessing slightly higher zero-shear-rate viscosity has also been characterized in detail by Hachmann [Hachmann & Meissner, 2003], The rheological properties for this latter grade have also been fitted to a multi-mode model appropriate for branched materials by Verbeeten et al. (2001). In order to avoid any rheological influences of the stabilizer package, and on the recommendation of Laun (2003), we have focused in the present work on the unstabilized Lupolen 1840H grade studied by Münstedt and coworkers [Gabriel *et al*. 1998; Münstedt *et al*. 1998].

It is well-known that low density polyethylene samples exhibit pronounced strain-hardening in transient uniaxial elongation and this can minimize the consequences of kinematic nonhomogeneities in fiber-windup devices [Connelly et al. 1979]. A more exacting test is thus provided by studying weakly strain-hardening materials such as linear low density polyethylene (LLDPE). Schulze et al. [2001] present a comparison of transient extensional stress growth data for a commercially available LLDPE (Dow Affinity PL1880) in a number of RME devices and also report corrected strain-rates that are determined independently from visual inspection of sample deformations. We thus perform corresponding measurements of the transient extensional rheology in LLDPE using the SER fixture.

We first describe the preparation and rheological characterization of the test samples. We then use two independent sets of SER test fixtures, mounted on a controlled rate and controlled stress instrument respectively, to measure the extensional stress growth in the LLDPE samples. We then turn our attention to the more strain-hardening LDPE materials. We investigate the tensile stress relaxation following imposition of a small Hencky strain, and then measure the onset of strain-hardening under steady uniaxial stretching conditions. We also demonstrate the ability to make tensile creep measurements in LDPE using the SER fixture mounted on a controlled stress rheometer and compare the results with the corresponding measurements of Münstedt et al. (1998). Finally we measure the relaxation of the tensile stresses following cessation of steady elongation over a range of imposed deformation rates, and observe sample

necking and viscoelastic failure at large strains. Finally we explore the viscoelastic nature of this failure condition in more detail using an ultrahigh molecular weight polyethylene sample.

II. Materials and Procedures

A. SER Fixture

Extensional rheological measurements were performed on a SER Universal Testing Platform (Xpansion Instruments LLC) specifically designed for use as a detachable extensional rheometer fixture on commercially-available torsional rheometer systems. Two different SER models were employed in the present work: (a) a model SER-HV-A01 was used on both a TA/Rheometrics ARES and an RDA-II rotational rheometer, and (b) a model SER-HV-P01 was used on an Anton Paar Physica MCR501 rotational rheometer host system. This device is a controlled stress instrument that can also be operated in a controlled-strain mode.

As shown in Figure 1, and described in detail by Sentmanat [Sentmanat, 2003a, 2003b; 2004], the SER consists of paired master and slave windup drums mounted on bearings housed within a chassis and mechanically coupled via intermeshing gears. Rotation of the drive shaft results in a rotation of the affixed master drum and an equal but opposite rotation of the slave drum which causes the ends of the sample that are secured to the drums by means of securing clamps to be wound up onto the drums resulting in the sample being stretched over an unsupported length, L_0. Axial sagging of the sample is inhibited by mounting the molten sheet of the test sample vertically, rather than horizontally as in the RME, and is not an issue for samples with zero-shear-rate viscosities in excess of 10^4 Pa s. A detailed analysis of the geometric requirements to be fulfilled in order to neglect sagging is provided in the appendix to Sentmanat [2004].

For a constant drive shaft rotation rate, Ω, a constant Hencky strain rate is applied to the sample specimen that can be expressed as:

$$\dot{\varepsilon}_{\mathrm{H}} = \frac{2\Omega R}{L_0} \tag{1}$$

where R is the radius of the equi-dimensional windup drums, and L_0 is the fixed, unsupported length of the specimen sample being stretched which is equal to the centerline distance between the master and slave drums. The resistance of the specimen to elongation is observed as a tangential force, F, acting on both the master and slave drums which is then manifested as a torque, $\mathcal{T}$, on the torque transducer attached to the fixture. It has been shown [Sentmanat, 2004]

that the measured torque signal, $\mathcal{T}'(t)$, is related to the tangential stretching force, F, in the following manner:

$$\mathcal{T}'(t) = 2RF(t). \tag{2}$$

This expression has been shown to be valid for measured torque values greater than $\mathcal{T}' \geq 4.0\times10^{-5}$ N m with bearing friction contributing less than 2% to the total measured torque signal.

For a constant Hencky strain rate experiment, the instantaneous cross-sectional area, $A(t)$, of a stretched molten specimen changes exponentially with time, t. Now although the width and thickness dimensions of the prepared polymer specimens were measured at room temperature prior to loading on the SER, the polymer samples exhibit a decrease in density upon melting that is manifested as a volumetric expansion of the specimen span while loaded on the SER. In order to account for this dimensional expansion, affine expansion of the sample is assumed and the following expression was used to calculate the cross-sectional area of the molten polymer specimen for a constant Hencky strain rate experiment:

$$A(t) = A_0\left(\frac{\rho_S}{\rho_M}\right)^{2/3}\exp\left[-\dot{\varepsilon}_H t\right] \tag{3}$$

where A_0 is the cross-sectional area of the specimen in the solid state, ρ_S is the solid state density and ρ_M the melt density of the polymer. Note that any expansion in the unsupported span length of the polymer is observed as a slight lag in the torque response that can be accounted for with a slight time offset in the recorded time data. For a constant Hencky strain rate, the tensile stress growth function, $\eta_E^+(t)$, of the stretched sample can then be expressed as:

$$\eta_E^+(t) = \frac{F(t)}{\dot{\varepsilon}_H A(t)}\ , \tag{4}$$

where $F(t)$ is the instantaneous extensional force exerted by the sample at time t as it resists stretching and as determined from the measured torque signal, $\mathcal{T}'(t)$, and Eq. 2.

In an extensional stress relaxation experiment with the SER, the tensile relaxation modulus, $E(t)$, of the stretched sample can be found from the expression:

$$E(t) = \frac{F(t)}{\varepsilon_H A(t)}, \tag{5}$$

where $F(t)$ is the instantaneous extensional force at time t exerted by the sample as it relaxes from the imposed step Hencky strain, $\varepsilon_H = 2R\Delta\theta/L$. Although this has historically been a very difficult measurement to perform with conventional extensional melt rheometer technology, the use of a standard torsional rheometer makes this achievable because the drive system has been designed with the ability to rapidly impose a step angular displacement, $\Delta\theta$.

In a tensile creep experiment at a constant stress $\sigma_0 = F(t)/A(t)$, the tensile force imposed on the sample must vary in the same manner that the cross-sectional area of the sample varies; i.e. it must decrease exponentially with Hencky strain. Hence, in order to perform constant tensile stress experiments with the SER, the torque of the MCR501 controlled stress rheometer is programmed in the firmware to decay exponentially with the angle of spindle rotation such that $\mathcal{T} = \mathcal{T}_0 \exp(-\varepsilon_H)$ where $\mathcal{T}$ is the applied torque, $\mathcal{T}_0$ is the initial applied torque (based on the desired tensile creep stress for a given initial cross-sectional area of the melt sample), and $\varepsilon_H(t) = 2R\Delta\theta(t)/L$ is the measured Hencky strain. The extensional creep compliance is then defined as $D(t,\sigma_0) \equiv \varepsilon_H(t)/\sigma_0$.

B. Sample Preparation

Sample specimens of LLDPE Affinity PL1880 (M_n = 36,000, M_w = 97,000, $\eta_0 = 7.9 \times 10^4$ Pa s @ 130°C) supplied by S. Costeux (Dow) and LDPE Lupolen 1840H (M_n = 17,000, M_w = 240,000, CH_3/1000C = 23, $\eta_0 = 5.9 \pm 0.3 \times 10^4$ Pa s @ 150°C) supplied by C. Gabriel (BASF) were prepared by compression molding approximately 7g of polymer pellets at a temperature of 150°C between smooth polyester film sheets to a nominal gage thickness of 0.65-1 mm. Sample thickness was controlled by using thin flat window frame molds of uniform gage, sandwiched between two flat steel platens. The samples were compression molded for a period of 10-15 minutes in a pre-heated hydraulic press and then removed and allowed to cool to room temperature by natural convection. Once the sample had cooled to room temperature, a long strip approximately 15-18 mm in width was cut from the flat molded sheet. Small rectangular specimens 12.7 mm in fixed width were then cut from the long strip section using a dual blade cutter with a fixed gap spacer. The final dimensions of the solid polymer specimens were approximately 17 mm in length × 12.7 mm in width, with thicknesses in the range of 0.65 —1 mm.

Prior to sample loading, the SER fixture was heated to the desired value (130˚C for LLDPE and 150°C for the LDPE tests) using the environmental chamber of the host system. Once the oven temperature had reached the set point, the fixture was allowed to soak at temperature for a minimum of 20 minutes prior to initial sample loading. The loading procedure involved opening the oven chamber door and using a pair of fine tweezers, loading and securing the specimen onto the preheated SER fixture, then closing the oven chamber door all within a time span of about 20-30 seconds. A period of about 90 seconds was allowed to elapse prior to starting a test in order to allow the oven and sample specimen to reach the test temperature.

The characteristic thermal diffusion time for sample equilibration may be estimated as $t_{diff} \approx \rho_M c_P h^2/k$ where h is the sample thickness and k, c_P are the thermal conductivity and

specific heat respectively. For 1mm thick samples, using published values for polyethylene (k = 0.241 W/mK; c_P = 2570 J/kgK, ρ_M = 0.782 g/cm^3) we find $t_{diff} = \rho_M c_P h^2 / k \approx 8.4 s$. The sample is thus well equilibrated within 90 seconds.

The measured density of both polyethylene samples at room temperature is ρ_s = 0.92 g/cm^3. In the melt state ($T \geq 136$°C), the density of all polyethylenes is reported to vary with temperature as $\rho_M(T) = \left[1.262 + 9.0 \times 10^{-4}\left(T - 125°C\right)\right]^{-1}$ with ρ_M in g/cm^3 [Meissner & Hostettler, 1994]. At a test temperature of 150°C, the correction factor in eq. (3) is thus $\left(\rho_s / \rho_M\right)^{2/3} = \left(0.78/0.92\right)^{2/3} \approx 1.12$.

At the end of a test, molten specimen remnants on the windup drum surfaces and securing clamps were immediately removed using a small scraping tool fashioned from brass shim stock. A representative image taken during an interrupted test with the oven doors open is shown in Figure 1. The hyperbolic shape of the material elements taken up by the rotating drums is evident. Once the majority of specimen remnants had been removed from the fixture, the windup drums were carefully wiped clean with a soft disposable laboratory wipe to remove any remaining residue off the drum surfaces.

III. RESULTS AND DISCUSSION

A. Transient Extensional Stress Growth of LLDPE

We first investigate the evolution in the transient extensional viscosity function $\eta_E^+(\dot{\varepsilon}_H, t)$ for the Affinity LLDPE. The data presented in Figure 2 were generated with a model SER-HV-P01 mounted on an Anton Paar MCR501 torsional rheometer using the controlled rate mode of operation. The solid line shows the linear viscoelastic envelope $\eta_E^+ = 3\eta^+$ obtained from start-up of steady shear experiments with a cone and plate fixture. Theoretical considerations show that this defines the LVE envelope of extensional flow behavior [Bird et al. 1987]. The zero-shear-rate viscosity of the Affinity sample can be determined from the long time asymptote of this curve to be $\eta_0 = 7.9 \times 10^4$ Pa s, in good agreement with Schulze et al. The tensile stress growth curves for the Affinity polyolefin exhibit little deviation from the linear viscoelastic envelope for extension rates $0.01 \leq \dot{\varepsilon}_H \leq 20 s^{-1}$ up to the maximum achievable Hencky strain of $\varepsilon_H = 4.5$. In Figure 3 we compare these measurements with the "corrected" extensional results reported in Figure 8 of the round-robin study of Schulze et al [2001]. Each curve is offset along the ordinate axis by one decade for clarity. The data were generated with 2 SER models: an SER-HV-P01 hosted an Anton Paar MCR501 and an SER-HV-A01 hosted on a Rheometrics RDA-II. In the SER design there is no relative slippage between the two counter-rotating rollers and the

samples; we do not correct the imposed deformation rate *a posteriori* but rather we directly specify rates of $\dot{\varepsilon}_H = 0.01, 0.095$, and $0.895 s^{-1}$ in order to enable direct comparison with Schulze et al. If desired, the homogeneity of the deformation can be verified by direct analysis of video frames because the fixture does not rotate during operation and representative data is presented elsewhere [Sentmanat, 2004]. At the highest extension rate of $\dot{\varepsilon}_0 = 0.895 s^{-1}$ a small amount of strain-hardening can be detected for Hencky strains $\varepsilon_H \geq 1$; however, in general, the extensional stress growth closely follows the linear viscoelastic envelope. The agreement of both sets of SER results with the LVE data at short times provide validation of the accuracy and reproducibility of the SER fixtures. By contrast, the RME results exhibit poor agreement (with up to a factor of two difference [Schulze et al. 2001]) with the equivalent LVE results at short times. This discrepancy is attributed by the authors to the belts taking up initial sample slack at times $t \leq 0.5$ seconds.

B. Shear Rheology of Lupolen 1840H

Having demonstrated the ability to measure the transient extensional viscosity of a very weakly strain-hardening material we now investigate a strongly-strain-hardening low density polyethylene. The steady and transient shear rheology of Lupolen 1840H has already been studied in great detail by Münstedt and co-workers [Gabriel *et al*., 1998; Münstedt *et al*. 1998]. Note that in these papers it is denoted as LDPE Melt I. Gabriel et al. point out that long relaxation modes are present in the material as a result of the long chain branching and also that this material (which does not contain a stabilizer package) is prone to thermal degradation at long times (in excess of 3600 seconds). Following this earlier study [Gabriel et al. 1998] we perform creep measurements at shear stresses of τ_0 = 1000, 100 and 10 Pa. At long times ($t \geq$ 500 s) the compliance is found to increase linearly with time and becomes independent of stress amplitude. The zero shear-rate viscosity of the sample can be computed from these measurements to be $\eta_0 = (5.9 \pm 0.3) \times 10^4$ Pa s in agreement with the published value of Gabriel et al.

By using the techniques described by Gabriel et al. (1998) and Kraft et al. (1999) – and which are now provided in modern software packages (TA Rheology Advantage ver 5.0.38) – it is possible to use the measured creep data to augment measurements in small amplitude oscillatory shear flow without the need for excessively long test durations. In Figure 4 we show the measured linear viscoelastic moduli of Lupolen 1840H at 150˚C together with the predicted values obtained from inverting a discrete retardation spectrum that was fitted to the creep data measured independently. The inset to Figure 4 also shows (on an expanded linear scale) the progressive change in the storage modulus measured at a single frequency of ω = 0.05 rad/s. After an induction period of approximately 3000 s the material functions begin to change with

increasing rapidity. For this reason all tests have been limited to durations of less than 1000 seconds. Small amplitude oscillatory shear flow experiments at temperatures $140 \le T \le 170$°C showed that before the onset of thermal degradation, the Lupolen samples obeyed the principles of time-temperature superposition with an Arrhenius activation energy of $E_a = 54.4$ kJ/mol.

C. Step Strain and the Relaxation Modulus of Lupolen 1840H

There has been recent interest in investigating the stress relaxation in entangled polymer systems following imposition of a step extensional strain [Barroso & Maia, 2002]. As a validation of the capabilities of the SER fixture in the linear viscoelastic (LVE) flow regime, extensional stress relaxation experiments for a step Hencky strain of $\varepsilon_H = 0.4$ were performed with the SER-HV-A01 on a Lupolen 1840H sample at a melt temperature of 150°C. This is the maximum step strain that can be imposed by the SER due to constraints imposed by the maximum angular displacement of the ARES motor ($\Delta\theta_{max} = 0.5$ rad). The resulting data for the tensile relaxation modulus (evaluated using Eq. 5) can be compared with the LVE shear stress relaxation results taken from cone & plate measurements in step shear. As shown in Figure 5, a plot of the tensile relaxation modulus, $E(t)$, exhibits excellent superposition with a plot of $3G(t)$ taken from the LVE shear stress relaxation data, and constitutes an experimental validation of Trouton's rule in stress relaxation mode.

D. Transient Extensional Viscosity Function

Start-up of steady extension experiments were performed on Lupolen 1840H at a melt temperature of 150°C and over a range of Hencky strain rates from 0.003 to 30 s^{-1}, as shown in Figure 6. Once again we compare results obtained using separate SER fixtures mounted on both an MCR and an ARES rheometer. Superposed with the tensile growth data is the LVE shear stress growth data, $3\eta^+(t)$, for Lupolen 1840H at 150°C taken from cone & plate measurements in start-up of steady simple shear flow. Data obtained at times $t \le 0.01$ s are not plotted for either shear or extensional tests as they are convolved with the response function of the rheometer motors plus any residual sag in the sample resulting from uncorrected thermal expansion. The agreement between the low strain portion of the tensile stress growth curves and the LVE simple shear data is noteworthy and provides experimental validation of the capabilities of the SER fixtures with regard to LVE flow characterization even for low deformation rates. The significant strain hardening exhibited in the tensile stress growth behavior at large strains is inherent with polymer melts such as LDPE that contain a high degree of long-chain branching.

Further validation of the extensional melt flow characterization capabilities of the SER are provided in Figure 7. Here we compare our tensile stress growth data with values taken from the literature [Münstedt et al., 1998] for the same Lupolen 1840H polymer (denoted Melt I therein) and the same melt temperature. Despite the different rheometer technologies utilized to collect the extensional data in Figure 7, the agreement in this transient extensional rheological data is remarkable, particularly when one considers that even factoring in the sample loading, heating, testing, clean-up, and re-heating time, the tensile stress growth data in Figure 6 took just over an hour to generate with the SER.

The original IUPAC A LDPE was synthesized more than three decades ago and some long term aging has resulted as a result of the absence of any stabilizer packages for free radical scavenging (Laun, personal communication 2003). The present test material, Lupolen 1840H, has been proposed as an equivalent LDPE polymer material with regard to melt flow behavior and polymer macrostructure. Figure 8 contains a comparison of tensile stress growth data at a melt temperature of 150°C for Lupolen 1840H generated with the SER and IUPAC A results taken from the literature [Münstedt & Laun, 1979]. The LVE stress growth envelope for IUPAC A was calculated from the integral of a Maxwell model fit of the discrete relaxation time spectra reported in the literature [Rauschenberger & Laun, 1997]. This model predicts a higher extensional viscosity at short times $t \leq 0.02$ s than is observed in the Lupolen data; however there is no extensional data available for IUPAC A at these short times to confirm or refute the model extrapolation.

Note that although the two polymers exhibit qualitatively similar tensile stress growth behavior, there is an apparent difference in LVE stress growth behavior which is also reflected in the zero-shear viscosities of Lupolen 1840H (η_0 = 5.9 ± 0.3 $\times 10^4$ Pa s) and IUPAC A ($\eta_0 = 5.2 \times 10^4$ Pa s). This difference suggests a slightly higher bulk average molecular weight for the Lupolen 1840H when compared to the IUPAC A material. Focusing on the large strain portion of the tensile stress growth curves, the data also suggest subtle differences in long-chain branching between the two polymers as witnessed by the slight variance in strain hardening behaviors, particularly at low rates of extension. This subtle difference in long-chain branching is further illustrated by the data in Figure 9 which provides a measure of the 'steady uniaxial extensional viscosity' behavior of the two polymers. Following earlier work, we evaluate this steady state value from the peak of the tensile stress growth curves as a function of Hencky strain rate shown in Figure 6, such that $\eta_E(\dot{\varepsilon}_H) = \max\left(\eta_E^+(\dot{\varepsilon}_H, t)\right)$. Although an extensional viscosity can still be computed beyond this point using the measured tensile force, the imposed deformation rate and the (assumed) exponential variation in the cross-sectional area, our stress relaxation experiments (see §III.F for details) coupled with theoretical and numerical stability considerations [Hassager et al. 1998; McKinley & Hassager, 1999] suggest that beyond the

maximum the elongating polymeric strip is in fact unstable to free surface perturbations that grow and result in necking of the sample, followed by complete rupture. The actual cross-sectional area and the local deformation rate in the neck will thus not be the same as the nominal imposed values. We therefore do not use the measured data beyond the maximum value of the transient extensional viscosity for representing the true steady-state extensional viscosity function.

Although the deviation from the limiting zero-deformation rate behavior in Figure 9 appears to begin at approximately the same deformation rate for both materials, the Lupolen 1840H exhibits significantly less extensional thickening than the IUPAC A at low to moderate extension rates. This behavior is consistent with the presence of a reduced number of long-chain branches and a proportionally larger number of long linear chains. This observation is also supported by the number of methyl groups per 1000 carbon atoms (CH_3/1000C) that has been reported in the literature for each polymer; 23 for Lupolen 1840H [Gabriel *et al.,* 1998] and 30 for IUPAC A [Laun & Schuch, 1989].

Using the SER fixture we were able to obtain tensile stress growth curves up to Hencky strain rates of $\dot{\varepsilon}_H = 30\text{s}^{-1}$. The associated values of the 'steady extensional viscosity' (as represented by the maximum in the transient extensional viscosity) at high deformation rates show extension thinning with an asymptotic slope close to $\eta_E \sim \dot{\varepsilon}_H^{-1/2}$. We discuss these observations further in §IV.

E. Tensile Creep Under Constant Stress

By controlling the imposed torque on the SER-HV-P01 it is also possible to impose a constant tensile stress on samples of the Lupolen material. As Münstedt et al. [1998] note, tensile creep experiments typically approach steady state conditions more rapidly and the steady uniaxial viscosity can thus be extracted from tensile creep data over a wide range of imposed stresses. In Figure 10 we show a representative comparison of the shear creep compliance $J(t)/3$ for Lupolen 1840H measured using an AR2000N rheometer at constant shear stresses of τ_0 = 10, 100 and 1000 Pa with the tensile creep compliance $D(t) = \varepsilon_H(t)/\sigma_0$ measured using the MCR501 in controlled torque mode. Good agreement between the data is obtained at all times $0.3 \le t \le 300$ s. At short times $t \le 0.1$ s, damped inertioelastic oscillations are observed in the torsional data as a result of the moment of inertia of the instrument [Arigo et al. 1997]. In Figure 11 we replot the measured Hencky strain $\varepsilon_H(t)$ at a constant tensile stress of σ_0 = 1000 Pa on a linear scale and compare it with the equivalent data reported by Münstedt et al. [1998]. Numerical differentiation of the Hencky strain gives the strain rate in the sample which asymptotes to a value of $\dot{\varepsilon}_H = d\varepsilon_H/dt = 0.045 \pm 0.005\,\text{s}^{-1}$ after times of 300 seconds. The imposed tensile stress and measured deformation rate can then be used to evaluate a steady

elongational viscosity which we show in Figure 12 as a function of the imposed tensile stress. We obtain excellent agreement with the data of Münstedt et al. for tensile stresses $10^3 \le \sigma_0 \le 10^5$ Pa.

F. Stress Relaxation Following Cessation of Stretching

The small moving mass of the SER fixture and the obviation of the need to impose an exponential increasing endplate velocity, as in a filament stretching rheometer, allows one to perform tensile stress relaxation experiments following elongation using the SER fixture. Cessation of steady extension rate experiments were performed on the Lupolen 1840H at a melt temperature of 150°C, an applied Hencky strain rate of 0.5 s^{-1}, and cessation times of t_0 = 1, 2, 3, 4, 5, and 6 seconds, respectively. The results of these experiments are shown in Figure 13. Included with the cessation data is the tensile growth curve for an uninterrupted strain rate test at the same Hencky strain rate of 0.5 s^{-1}. Also depicted in Figure 13 is the LVE prediction of tensile stress growth and decay following the cessation of flow at a time, t_0 = 1 s (corresponding to a Hencky strain $\varepsilon_H = 0.5$) calculated from the following expressions:

$$\text{for } t \le t_0 \qquad \eta_E^+(t) = 3\int_0^t G(t)dt \tag{6}$$

$$\text{for } t > t_0 \qquad \eta_E^-(t) = 3\int_{t-t_0}^t G(t)dt \tag{7}$$

where $G(t)$ is the linear viscoelastic shear relaxation modulus. The superposition between the LVE stress growth and decay predictions and the SER tensile data for cessation of flow at t_0 = 1 second is noteworthy. In addition, the superposition of all the tensile stress growth data in Figure 13 provides a measure of the excellent experimental reproducibility that can be achieved with the SER.

The final stress relaxation curve shown in Figure 13, corresponding to the cessation of extension at a time of t_0 = 6.0 seconds (ε_H = 3), exhibits an unexpectedly rapid decay in the tensile stress at long times. Inspection of the melt sample showed that it exhibited a subtle ductile necking phenomenon; the stretched sample continued to become progressively thinner in the region between the opposing rollers, whilst elastically unloading and recoiling near each roller. By contrast, all other samples remained homogeneous and continuous on the time scale of the experiments shown. Using the SER-HV-P01 fixture on the MCR501 we are also able to perform similar tensile stress relaxation experiments at short times and very high deformation rates as shown in Figure 14. We observe very similar behavior to that shown in Figure 14. Homogeneous relaxation is observed following stretching up to a maximum strain of $\varepsilon_H = (10)(0.25) = 2.5$;

however for larger initial imposed stretches a more rapid stress unloading and sample non-uniformity results.

The onset of this necking instability and ultimate failure of the sample can be interpreted within the framework of the Considère criterion [Malkin & Petrie, 1997; McKinley and Hassager, 1999]. In the rapid stretching limit corresponding to large Deborah numbers ($De >> 1$), dissipative losses in a viscoelastic material become negligible. The Considère criterion can then be expressed in the following form; for uniform elongation of a sample to be possible, the engineering stress $F(t)/A_0$ must be monotonically increasing. This expression can also be re-expressed as requiring that the extensional viscosity must be sufficiently strain-hardening that it increases at least exponentially with the Hencky strain; corresponding to $d\ln\eta_E^+/d\varepsilon \geq 1$ [McKinley & Hassager, 1999]. A closer inspection of the transient extensional viscosity data in Figures 6, 13 and 14 shows that indeed necking failure in the sample occurs very shortly after the transient extensional viscosity ceases to strain-harden exponentially fast.

For a viscoelastic material, the rate of necking following onset of instability is of course more complex than described by the purely-elastic Considère criterion [Joshi & Denn, (2004)]. In particular the growth rate of the necking disturbance in the sample profile will be dependent on exactly how the tensile stress evolves with deformation rate and Hencky strain in the material [McKinley, (2005)]. This can be seen more clearly in Figure 15(a) in which we replot the experimental measurements in terms of the *engineering stress;*

$$\frac{F(t)}{A_0} \equiv \eta_E^+ \dot{\varepsilon}\ \exp\left(-\varepsilon_H\right). \tag{8}$$

The dimensionless times (or Hencky strains) $\varepsilon_H = \dot{\varepsilon}\, t_0$ at which the stress relaxation experiments in Figures 13 & 14 were commenced are also indicated by the large open circles. It is clear that the onset of necking instability is connected with the rapid decrease in the engineering stress at high strains: beyond a Hencky strain $\varepsilon_H \approx 3$ the stress decreases rapidly at either value of the imposed strain rates and it is energetically cheaper for the portions of the sample away from the end-rollers to neck down and rupture. Similar responses have been seen in numerical simulations of filament stretching experiments at high *De* using both integral and differential viscoelastic constitutive equations [Hassager et al. 1998; Yao et al. 1998]. These simulations also show that the rate of elastic unloading and necking failure is mediated by the presence and magnitude of any 'solvent' contributions to the total stress arising from a true Newtonian solvent, a plasticizer or unentangled oligomer.

To explore the predictions of the Considère criterion further it is desirable to perform tests in the rapid stretching limit (corresponding to $De >> 1$) with highly entangled linear polymers. We have thus performed some preliminary experiments with an ultrahigh molecular

weight (UHMWPE) polyethylene sample. The UHMWPE has a molecular weight in excess of 10^6 g/mol and the mechanical properties at room temperature have been characterized by Pavoor (2003). As a consequence of the low entanglement molecular weight of polyethylene ($M_e \approx 828$ g/mol), UHMWPE is a very highly entangled and stiff rubbery material even at test temperatures of 200˚C. Few measurements of the melt rheological properties have been published. Okamato *et al*. (1998) have studied the transient extensional rheology of LDPE/UHMWPE blends and demonstrate that strain-hardening is still observed and that the stress-optical rule remains valid in the blends up to high extension; however they only consider blends containing from 1% to 10% UHMWPE. Recently Wang *et al*. (2003) reported measurements of the linear viscoelastic properties of 100% UHMWPE (in addition to Kaolin-filled samples) and documented the onset of slip-related instabilities in capillary extrusion.

In Figure 15(b) we show measurements of the engineering stress of an UHMWPE sample at T = 200˚C over a range of imposed stretch rates. Very large tensile stresses are achieved at small strains; however, the samples show a rapid rupture-like failure at Hencky strains of less than unity. In contrast to the measurements with the LDPE melt (also shown in Figure 15b for comparative purposes), very little strain-rate sensitivity can be detected in the tensile stresses measured in the UHMWPE samples indicating the approach to the 'rapid-stretching' elastic limit ($De \to \infty$). Finally we also show in Figure 15(b) the predictions of the Doi-Edwards theory (broken lines). In the rapid-stretching limit, the engineering stress for the Doi-Edwards model is given by the following expression [McKinley & Hassager, 1999]:

$$\frac{F(t)}{A_0} = \frac{5G_N^0}{2\lambda\left(\lambda^3 - 1\right)}\left[2\lambda^3 + 1 - 3\lambda^3 \frac{\tan^{-1}\left(\sqrt{\lambda^3 - 1}\right)}{\sqrt{\lambda^3 - 1}}\right], \tag{9}$$

where the axial stretch is $\lambda = \exp(\varepsilon_H)$ and G_N^0 is the Plateau modulus of the melt. The engineering stress passes through a maximum value of approximately $1.11\,G_N^0$ at a Hencky strain of $\varepsilon_{H,\max} = 0.86$.

For comparison of this theoretical prediction with the UHMWPE sample we use the accepted literature value of the plateau modulus for polyethylene; $G_N^0 = 2.6 \times 10^6$ Pa [Larson 1999]. For the Lupolen melt which contains a broad distribution of linear and branched chains this is not an appropriate value. Instead we experimentally determine the Plateau modulus using the relationship $d\eta^+/dt\Big|_{t=0} = G_N^0$ that can be derived from linear viscoelastic theory for small deformation rates. From the linear viscoelastic envelope in Figure 6 we thus obtain $G_N^0 = (5.0 \pm 0.1) \times 10^4$ Pa. In the case of the UHMWPE sample, the Doi-Edwards model provides a reasonably accurate upper bound to the experimental data and rupture is always

observed at critical strains $\varepsilon_{crit} \leq \varepsilon_{H,\max}$. For the Lupolen samples, the Doi-Edwards model provides a quantitative description of the initial stress growth in the material; however, the additional strain-hardening resulting from the branched molecules results in a significant increase in the engineering stress and also in the resulting strain to failure.

Finally, we show in Figure 16 the experimental data for the UHMWPE material plotted in terms of the transient extensional viscosity, computed using Eq. (8). Because the engineering stress is bounded and almost rate-independent, the evolution in the transient extensional viscosity is then dominated by the exponential decay in the cross-sectional area. As noted by Okamoto [Okamoto et al., 1998], the transient extensional viscosity can be described approximately by a polynomial $\eta_E^+ \sim t^n$. For the present UHMWPE, the data in Figure 11 suggests that $n \approx 0.8$. The extensional viscosity increases monotonically without bound until the point of rupture and it is not possible to attain a steady extensional viscosity in this material for any deformation rate.

IV. Conclusions

In this paper we have demonstrated that the SER Universal Testing Platform enables accurate and reproducible measurements of the transient extensional functions of viscoelastic samples such as polymer melts. We have performed tensile step strain, stress growth, tensile creep and stress relaxation experiments using both a linear low density polyethylene (Dow Affinity PL 1880) and a low density polyethylene sample (Lupolen 1840H). Comparisons with published data for both materials show very good agreement over a wide range of imposed strain rates. Additional testing experience [Sentmanat, 2004] shows that the SER test fixture can readily be used with stiffer materials such as elastomers and rubbers and also with lower viscosity materials; provided the zero-shear-rate viscosity at test temperature is bigger than approximately $\eta_0 \geq 10^4$ Pa s.

The transient tensile stress growth experiments coupled with subsequent stress relaxation experiments following cessation of stretching have shown that the LDPE samples become unstable to necking perturbations beyond a critical Hencky strain. The driving mechanism for this necking can be represented more clearly by examining the engineering stress that develops in the sample during stretching as shown in Figure 15. Earlier calculations [McKinley & Hassager 1999] of the Considère criterion with the Doi-Edwards model and also with the Pom-Pom model of McLeish and Larson (1998) have shown that it is the presence of long chain branching in the Lupolen samples that provides the plateau in the engineering stress at intermediate strains $1 \leq \varepsilon_H \leq 3$ and retards the onset of sample rupture. In the rapid stretching limit, the portion of the chain backbone between branches deforms affinely, and the branches act as true cross-links until the process of branch-point withdrawal commences. This stabilizing

process is absent in well-entangled linear melts, and analytic computation of the extensional stress for the Doi-Edwards model [McKinley & Hassager, 1999] suggests that the engineering stress passes through a single maximum and then decays exponentially. The material becomes unstable to further elongation at moderate Hencky strains of less than unity. This situation was anticipated by Doi & Edwards (1979) and is supported by our observations of stress growth and rupture in UHMWPE. Such tensile stress growth measurements have also been used in materials selection considerations [Pearson & Connelly, 1982].

Our transient elongational measurements with linear low density polyethylene (LLDPE) grades show much less strain-hardening than LDPE [Meissner and Hostettler, 1994; Münstedt et al. 1998]. They also exhibit lower elastic recoverable strain and may also develop inhomogeneities at smaller strains. The rate of ductile necking in these materials, however, is much less rapid than the elastic rupture we observed in the UHMWPE samples due to the viscous contributions to the stress. In such situations the Considère criterion does not provide a good measure of the strain to failure. Linear stability calculations [Hutchinson & Obrecht, 1977] and numerical simulations of filament stretching experiments [Hassager et al. 1998; Yao et al. 1999] show that these viscous contributions to the total tensile stress can have a significant impact on the ductile necking rate and the total strain required to achieve complete sample failure.

We are able to obtain curves of the steady state elongational viscosities for the LDPE samples either by imposing controlled extension rates or by tensile creep experiments at constant extensional stress. To be consistent with previous experimental measurements using low density polyethylenes, we have taken the maximum value of the measured transient extensional viscosity curve as the 'steady state' value of the ideal uniaxial extensional viscosity at that strain rate. The measurements shown in Figure 9 suggest that $\eta_E(\dot{\varepsilon}_H) \sim \dot{\varepsilon}_H^{-0.5}$ at high deformation rates. A similar power law decay at high strain rates has recently been noted by Bach & Hassager (2003) using a monodisperse polystyrene melt. Of course, the polystyrene data does not show the initial increase in the extensional viscosity observed in Figure 9 due to the absence of long chain branching.

The origins of this power-law decay in the extensional viscosity are not completely resolved. Reptation-based models such as the Doi-Edwards and Pom-Pom models predict a saturation in the tensile stress (occurring respectively when the chains reach full orientation or when branch-point withdrawal commences). The corresponding steady-state extensional viscosity then decreases as $\dot{\varepsilon}_H^{-1}$. By contrast, dumbbell-based viscoelastic constitutive models incorporating finite chain extensibility and anisotropic drag do predict the initial extensional thickening (resulting from chain stretching) followed by power-law thinning at a rate $\dot{\varepsilon}_H^{-1/2}$ as a result of molecular alignment and anisotropic frictional drag on the elongated chain [Wiest,

1989]. The physical mechanisms that would lead to anisotropic drag on highly elongated polymer chains are expected to be valid whether or not the material is entangled under equilibrium conditions. Such a view point is supported by filament stretching experiments in polymer solutions at high deformation rates: when the molecules are close to full stretch, measurements show that the steady-state extensional viscosity in dilute polystyrene solutions also decreases at a rate $\eta_E \sim \dot{\varepsilon}_H^{-1/2}$ [McKinley & Sridhar, 2002].

An alternate interpretation has been put forward recently by Marrucci & Ianniruberto (2004). They have considered in detail the deformed shape of the 'tube' in the reptation model and the resulting interchain pressure exerted on an elongated chain by the surrounding chains. The resulting model also predicts a power-law extensional thinning with a slope of –1/2. Measurements of the transient stress growth and approach to ultimate steady state elongational viscosity under both constant stress and constant rate conditions are greatly facilitated using the SER extensional test fixture. It is hoped that subsequent experiments with other monodisperse polymer melts will enable such phenomena to be investigated in greater detail in the future.

Acknowledgments.

The authors would like to thank Prof. R.E. Cohen for stimulating conversations on the topic of extensional rheology testing. We would also like to thank J. Dise & P. Pavoor for preparing the UHMWPE samples. This research was supported in part by the U.S. Army through the Institute for Soldier Nanotechnologies, under Contract DAAD-19-02-D0002 with the U.S. Army Research Office.

REFERENCES

Anna, S.L., McKinley, G.H., Nguyen, D.A., Sridhar, T., Muller, S.J., Huang, J. and James, D.F., An Inter-Laboratory Comparison of Measurements from Filament-Stretching Rheometers Using Common Test Fluids, *J. Rheol.*, **45**(1), 83-114 (2001).

Arigo, M.T. and McKinley, G.H., The Effects of Viscoelasticity on the Transient Motion of a Sphere in a Shear-Thinning Fluid, *J. Rheol.*, **41**(1), 103-128 (1997)**.**

Bach, A., Almdal, K., Rasmussen, H.K. and Hassager, O., Elongational Viscosity of Narrow Molar Mass Distribution Polystyrene, *Macromol.*, **36**(14), 5174-5179 (2003).

Barroso, V.C. and Maia, J.M., Evaluation by Means of Stress Relaxation (after a Step Strain) Experiments of the Viscoelastic Behavior of Polymer Melts in Uniaxial Extension, *Rheol. Acta*, **41**(3), 257-264 (2002).

Bird, R.B., Armstrong, R.C. and Hassager, O., Dynamics of Polymeric Liquids. Volume 1: Fluid Mechanics, Vol. 1, 2nd Edition, Wiley Interscience, New York, 1987.

Connelly, R.W., Garfield, L.J. and Pearson, G.H., Local Stretch History of a Fixed-End-Constant-Length-Polymer-Melt Stretching Experiment, *J. Rheol.*, **23**(5), 651-662 (1979).

Doi, M. and Edwards, S.F., Dynamics of concentrated polymer systems. IV. Rheological Properties, *J. Chem. Soc. Faraday Trans. II*, **75**, 38-54 (1978).

Gabriel, C, Kaschta, J. and Münstedt, H., "Influence of molecular structure on rheological properties of polyethylenes. I. Creep recovery measurements in shear," *Rheol. Acta*, **37**, 7-20 (1998).

Hachmann, P. and Meissner, J., Rheometer for Equibiaxial and Planar Elongations of Polymer Melts, *J. Rheol.*, **47**(4), 989-1010 (2003).

Hassager, O., Kolte, M.I. and Renardy, M., Failure and Nonfailure of Fluid Filaments in Extension, *J. Non-Newt. Fluid Mech.*, **76**(1-3), 137-152 (1998).

Hutchinson, J.W. and Obrecht, H., Tensile Instabilities in Strain-Rate Dependent Materials, *Fracture 1977 (ICF4)*, Waterloo, Canada, June 19-24, 1977, Vol.1, 101-116.

James, D.F. and Walters, K., "A Critical Appraisal of Available Methods for the Measurement of Extensional Properties of Mobile Systems", Techniques in Rheological Measurement, A. A. Collyer (ed.), Elsevier, London, 1993, 33-53.

Joshi, Y.M. and Denn, M.M., "Failure and Recovery of Entangled Polymer Melts in Elongational Flow", Rheology Reviews 2004, D. M. Binding, Walters,K. (eds.), British Society of Rheology, Aberystwyth.

Kraft, M., Meissner, J. and Kaschta, J., Linear Viscoelastic Characterization of Polymer Melts with long Relaxation Times, *Macromol.*, **32**, (1999), 751-757.

Larson, R.G., The Structure and Rheology of Complex Fluids, Topics in Chemical Engineering, Oxford University Press, New York, 1999.

Laun, H.M. and Münstedt, H., Comparison of the Elongational Behavior of a Polyethylene Melt at Constant Stress and Constant Strain Rate, *Rheol. Acta*, **15**(10), 517-524 (1979).

Laun, H.M., and Schuch, H., "Transient elongational viscosities and drawability of polymer melts," *J. Rheol.*, **33**, 119-175 (1989).

Laun, H.M., personal communication (2003).

Macosko, C. and Lorntson, J., The Rheology of Two Blow-Molding Polyethylenes, *SPE Tech Papers*, **19**, 461-467 (1973).

Malkin, A.Y. and Petrie, C.J.S., Some Conditions for Rupture of Polymeric Liquids in

Extension, *J. Rheol.*, **41**(1), 1-25 (1997).

Marrucci, G. and Ianniruberto, G., Interchain Pressure Effect in Extensional Flows of Entangled Polymer Melts, *Macromol.*, **37**(10), 3934-3942 (2004).

McKinley, G.H. Stretched to Breaking Point; Transient Extensional Rheology from the Melt to the Dilute Solution; Paper PL1, Society of Rheology Annual Meeting, Lubbock, Texas; Jan. 13-17, 2005.

McKinley, G.H. and Hassager, O., The Considère condition and Rapid Stretching of Linear and Branched Polymer Melts, *J. Rheol.*, **43**(5), 1195-1212 (1999).

McKinley, G.H. and Sridhar, T., "Filament Stretching Rheometry of Complex Liquids", Ann. Rev. Fluid Mech.,Vol.34, Annual Reviews Press, Palo Alto, 2002, 375-415.

McLeish, T.C.B. and Larson, R.G., Molecular Constitutive Equations for a Class of Branched Polymers: The Pom-Pom Model, *J. Rheol.*, **42**(1), 81-110 (1998).

Meissner, J., Experimental Aspects in Polymer Melt Elongational Rheology, *Chem. Eng. Commun.*, **33**, 159-180 (1985).

Meissner, J. and Hostettler, J., A New Elongational Rheometer for Polymer Melts and Other Highly Viscoelastic Liquids, *Rheol. Acta*, **33**(1), 1-21 (1994).

Münstedt, H and Laun H.M., Elongational behavior of a low density polyethylene melt. II. Transient behavior in constant stretching rate and tensile creep experiments. Comparison with shear data. Temperature dependence of the elongational properties, *Rheol. Acta*, **18**, 492-504 (1979).

Münstedt, H., New Universal Extensional Rheometer for Polymer Melts. Measurements on a Polystyrene Sample, *J. Rheol*, **24**(6), 847-867 (1979).

Münstedt, H, and Laun H.M., "Elongational properties and molecular structure of polyethylene melts," *Rheol. Acta*, **20**, 211-221 (1981)

Münstedt, H, Kurzbeck, S. and Egersdörfer, L., "Influence of molecular structure on rheological properties of polyethylenes – Part II: Elongational behavior," *Rheol. Acta*, **37**, 21-29 (1998)

Okamoto, M., Kojima, A. and Kotaka, T., Elongational Flow and Birefringence of Low Density Polyethylene and its Blends with Ultrahigh Molecular Weight Polyethylene, *Polymer*, **39**(11), 2149-2153 (1998).

Pavoor, P.V. ""Tribological and Mechanical Characterization of Polyelectrolyte Multilayer Nanoassemblies", MIT Ph.D./CEP Thesis. 2003.

Padmanabhan, M., Kasehagen, L.J. and Macosko, C., Transient Extensional Viscosity from a Rotational Shear Rheometer using Fiber-Windup Technique, *J. Rheol.*, **40**(4), 473-481 (1996).

Pearson, G.H. and Connelly, R.W., The use of Extensional Rheometry to Establish Operating Parameters for Stretching Processes, *J. Appl. Polym. Sci.*, **27**, 969-981 (1982).

Rauschenberger, V and Laun H.M., "A recursive model for Rheotens tests," *J. Rheol.*, **41**, 719-737 (1997)

Schulze, J.S., Lodge, T.P., Macosko, C.W., Hepperle.J., Munstedt, H., Bastian, H., Ferri, D., Groves, D.J., Kim, Y.-H., Lyon, M., Schweizer, T., Virkler, T., Wassner, E. and Zoetelief, W., A Comparison of Extensional Viscosity Measurements from Various RME Rheometers, *Rheol. Acta*, **40**, 457-466 (2001).

Schweizer, T., The Uniaxial Elongational Rheometer RME - Six Years of Experience, *Rheol. Acta*, **39**(5), 428-443 (2000).

Sentmanat, M.L., "A novel device for characterizing polymer flows in uniaxial extension," ANTEC '03, Soc. Plastics Engineers, Tech. Papers, 49, CD-ROM, New York (2003a).

Sentmanat, M.L., "Dual windup extensional rheometer," US Patent No. 6,578,413 (2003b).

Sentmanat, M.L., Miniature Universal Testing Platform: From Extensional Melt Rheology to Solid-State Deformation Behavior, *Rheol. Acta*, **43**, 657-669 (2004).

Sridhar, T., An Overview of the Project M1, *J. Non-Newtonian Fluid Mech.*, **35**, 85-92 (1990).

Verbeeten, W.M.H., Peters, G.W.M. and Baaijens, F.P.T., Differential Constitutive Equations for Polymer Melts: The Extended Pom-Pom Model, *J. Rheol.*, **45**(4), 823-843 (2001).

Wang, X., Wu, Q. and Qi, Z., Unusual Rheology Behavior of Ultra High Molecular Weight Polyethylene/Kaolin Composites Prepared via Polymerization-Filling, *Polym. Int.*, **52**, 1078-1082 (2003).

Wiest, J.M., A Differential Constitutive Equation for Polymer Melts, *Rheol. Acta*, **28**, 4-12 (1989).

Yao, M., McKinley, G.H. and Debbaut, B., Extensional Deformation, Stress Relaxation and Necking Failure of Viscoelastic Filaments, *J. Non-Newtonian Fluid Mech.*, **79** (Special Issue dedicated to 60th birthday of M. Crochet), 469-501 (1998).

FIGURE CAPTIONS

Figure 1: Photos of the SER Universal Testing Platform, from left to right; (a) the model SER-HV-A01, (b) a polyolefin melt sample being stretched during an extensional rheology measurement, and (c) the model SER-HV-P01.

Figure 2: Tensile stress growth curves at a melt temperature of 130°C for Affinity PL1880 LLDPE from Dow Chemical over a range of Hencky strain rates from $0.01s^{-1}$ to 20 s^{-1} generated with the SER. Also shown is the linear viscoelastic envelope (LVE) given by $\eta_E^+ = 3\eta^+$ obtained from cone and plate measurements in start-up of steady shear flow at $\dot{\gamma} = 0.003s^{-1}$.

Figure 3: Tensile stress growth data at a melt temperature of 130°C for Affinity PL1880 over a range of Hencky strain rates from 0.01 to 0.895 s^{-1} generated with the SER on two different host platforms, an MCR501 and RDA-II (light colored symbols and solid lines). The data are compared with extensional data taken from the literature (dark symbols from Schulze et al., 2001). Also shown is the linear viscoelastic envelope reported by Schulze et al. (light grey line), as well as our measurements of the linear viscoelastic response (black dotted line) given by $\eta_E^+ = 3\eta^+$ obtained from cone and plate measurements in start-up of steady shear flow at $\dot{\gamma} = 0.003s^{-1}$.

Figure 4. The linear viscoelastic moduli (G′(ω) and G″(ω)) for Lupolen 1840H at 150°C. Solid lines are calculated from creep measurements and the computed retardation spectrum, and the symbols are from small amplitude oscillation experiments. The inset data shows the thermal stability of LDPE at 150°C and the progressive change in the modulus for test times in excess of 3000 seconds.

Figure 5: Tensile stress relaxation modulus at a melt temperature of 150°C for Lupolen 1840H obtained from a step strain experiment with the SER to a Hencky strain of ε_H = 0.4 and a plot of $3G(t)$ using shear relaxation modulus data obtained from cone and plate measurements in a step shear experiment.

Figure 6: Tensile stress growth curves at a melt temperature of 150°C for Lupolen 1840H over a range of Hencky strain rates from 0.003 to 30 s^{-1} generated with the SER on two different host platforms, an MCR501 and an ARES, and a plot of LVE $3\eta^+$ shear stress growth data taken from cone and plate measurements in start-up of steady shear at a shear rate of 0.005 s^{-1}.

Figure 7: Comparison of tensile stress growth data at a melt temperature of 150°C for Lupolen 1840H over a range of Hencky strain rates from 0.003 to 1 s^{-1} generated with the SER on two different host platforms (solid lines) with extensional data taken from the literature (symbols with lines from Münstedt, 1998).

Figure 8: Comparison of tensile stress growth data at a melt temperature of 150°C over a range of Hencky strain rates from 0.003 to 30 s^{-1} for Lupolen 1840H generated with the

SER (solid lines) and for IUPAC A taken from the literature (symbols from Münstedt & Laun, 1979).

Figure 9: Comparison of the steady-state extensional viscosity behavior as a function of Hencky strain rate at a melt temperature of 150°C for Lupolen 1840H generated with the SER (triangles) and for IUPAC A taken from the literature (circles from Münstedt & Laun, 1979).

Figure 10: Comparison of shear creep compliance measurements for Lupolen 1840H from BASF at three stresses (150^{o}C) with tensile creep compliance measurements generated with the SER on a MCR501 host platform.

Figure 11: Comparison of tensile creep compliance data at a melt temperature of 150°C for Lupolen 1840H at a tensile creep stress of 1000 Pa generated with the SER (symbols) with tensile creep compliance data taken from the literature (solid lines from Münstedt, 1998).

Figure 12: Comparison of steady-state extensional viscosity η_E (scaled with $3\eta_0$) as a function of the imposed tensile creep stress at a melt temperature of 150°C for Lupolen 1840H generated with the SER (diamond symbols) with data taken from the literature (square symbols from Münstedt, 1998).

Figure 13: Cessation of steady extension rate experiments at a melt temperature of 150°C for Lupolen 1840H at a Hencky strain rate of 0.5 s^{-1} and cessation times, t_0, (from bottom to top) of 1, 2, 3, 4, 5, and 6 seconds.

Figure 14: Cessation of steady extension rate experiments at a melt temperature of 150°C for Lupolen 1840H at a Hencky strain rate of 10 s^{-1} and cessation times, t_0, (from bottom to top) of 0.10, 0.15, 0.20, 0.25, 0.30, and 0.35 seconds.

Figure 15: Evolution of the engineering tensile stress with Hencky strain over a range of Hencky strain rates: (a) data for Lupolen 1840H at a melt temperature of 150°C at Hencky strain rates of 0.5 and 10 s^{-1}. The large open circles indicate the Hencky strains at which the stress relaxation experiments were performed. (b) Comparison with data for UHMWPE at a melt temperature of 200°C. The broken lines show the predictions of the Doi-Edwards theory in the rapid stretching limit (see Eq. 9).

Figure 16. The transient extensional viscosity of an UHMWPE melt tested in the SER. The extensional viscosity continues to grow without bound at all extension rates until onset of necking instability and the sample ruptures.

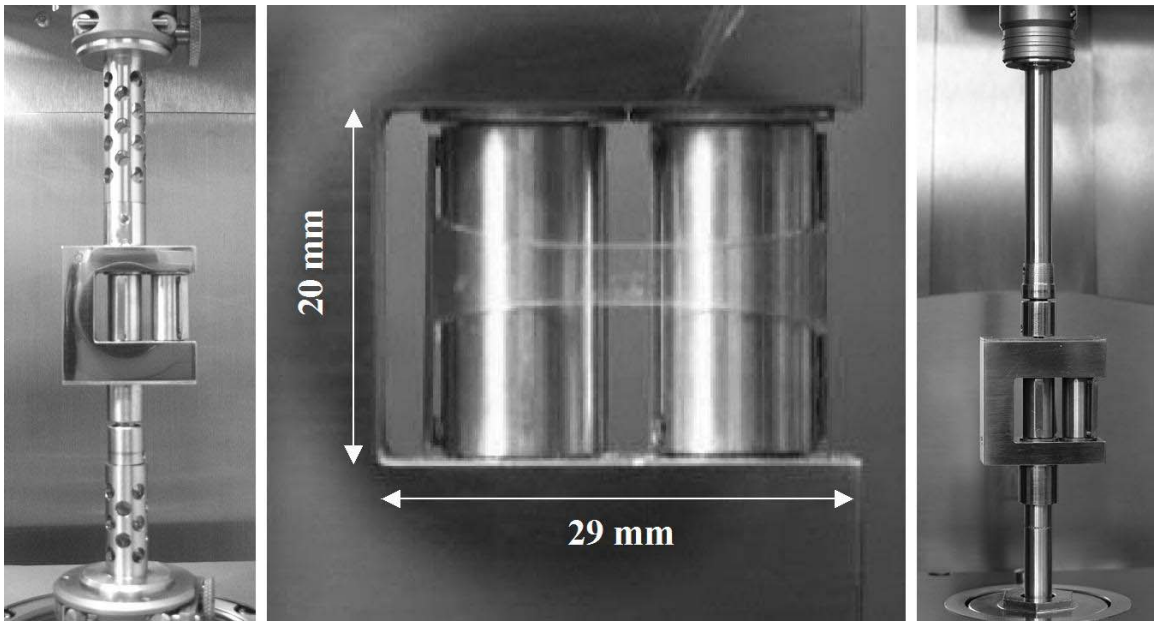

Figure 1: Photos of the SER Universal Testing Platform, from left to right; (a) the model SER-HV-A01, (b) a polyolefin melt sample being stretched during an extensional rheology measurement, and (c) the model SER-HV-P01.

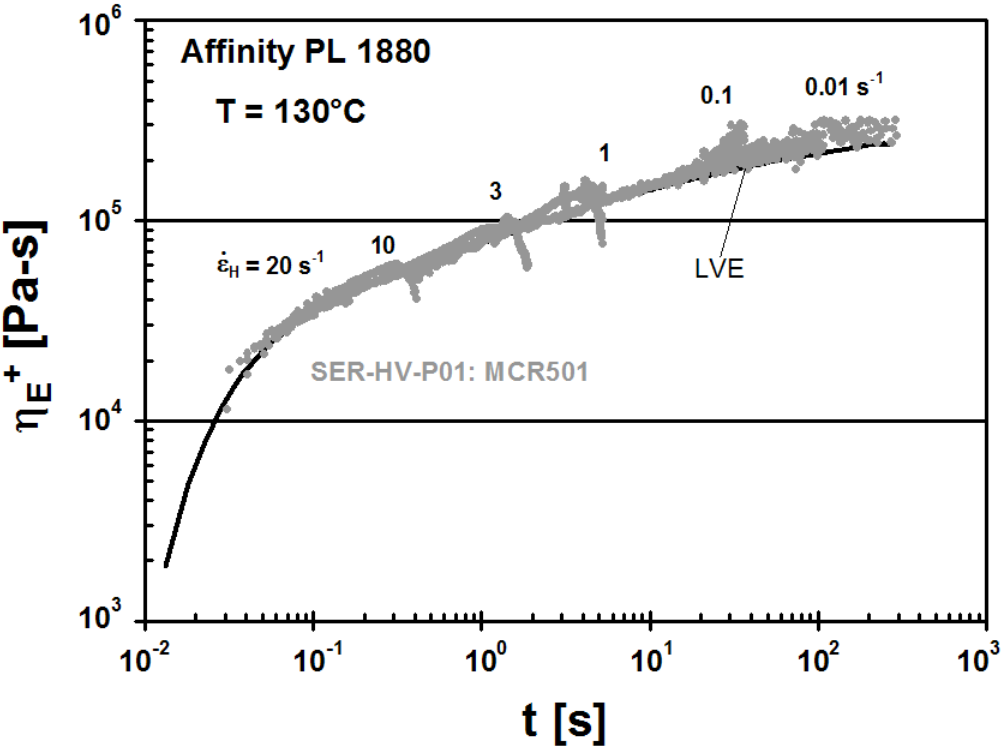

Figure 2: Tensile stress growth curves at a melt temperature of 130°C for Affinity PL1880 LLDPE from Dow Chemical over a range of Hencky strain rates from $0.01s^{-1}$ to 20 s^{-1} generated with the SER. Also shown is the linear viscoelastic envelope (LVE) given by $\eta_E^+ = 3\eta^+$ obtained from cone and plate measurements in start-up of steady shear flow at $\dot{\gamma} = 0.003s^{-1}$.

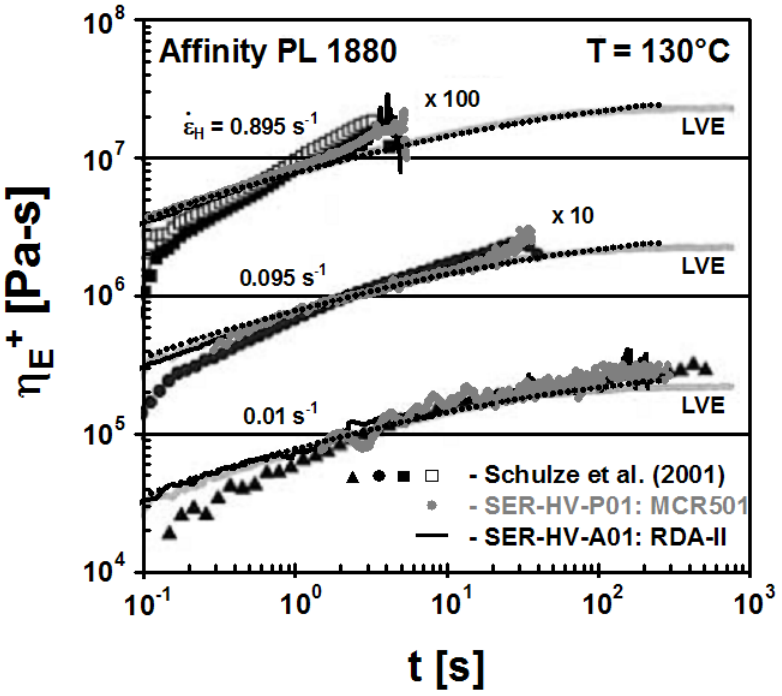

Figure 3: Tensile stress growth data at a melt temperature of 130°C for Affinity PL1880 over a range of Hencky strain rates from 0.01 to 0.895 s^{-1} generated with the SER on two different host platforms, an MCR501 and RDA-II (light colored symbols and solid lines). The data are compared with extensional data taken from the literature (dark symbols from Schulze et al., 2001). Also shown is the linear viscoelastic envelope reported by Schulze et al. (light grey line), as well as our measurements of the linear viscoelastic response (black dotted line) given by $\eta_E^+ = 3\eta^+$ obtained from cone and plate measurements in start-up of steady shear flow at $\dot{\gamma} = 0.003 s^{-1}$.

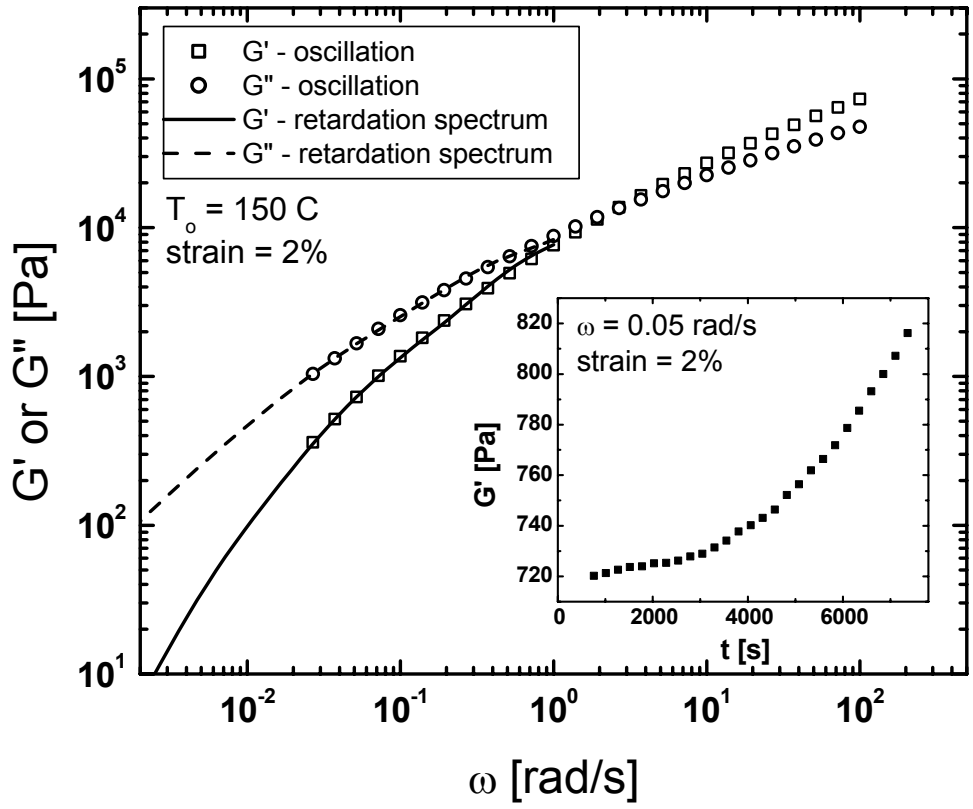

Figure 4. The linear viscoelastic moduli ($G'(\omega)$ and $G''(\omega)$) for Lupolen 1840H at 150°C. Solid lines are calculated from creep measurements and the computed retardation spectrum, and the symbols are from small amplitude oscillation experiments. The inset data shows the thermal stability of LDPE at 150°C and the progressive change in the modulus for test times in excess of 3000 seconds.

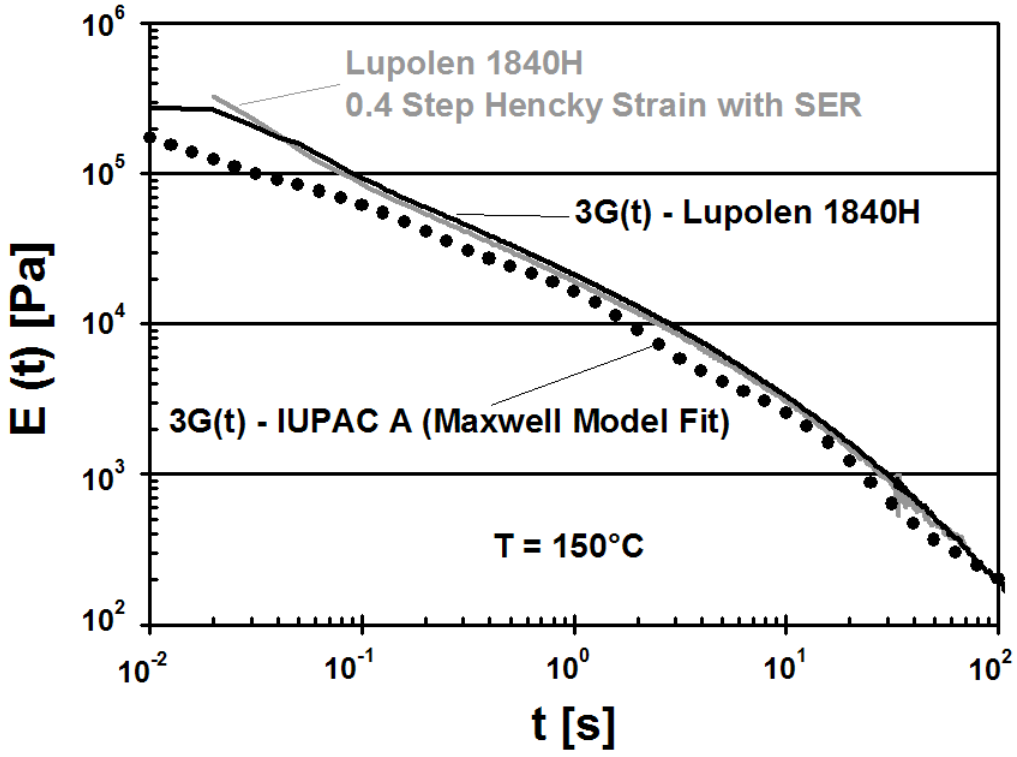

Figure 5: Tensile stress relaxation modulus at a melt temperature of 150°C for Lupolen 1840H obtained from a step strain experiment with the SER to a Hencky strain of ε_H = 0.4 and a plot of $3G(t)$ using shear relaxation modulus data obtained from cone and plate measurements in a step shear experiment.

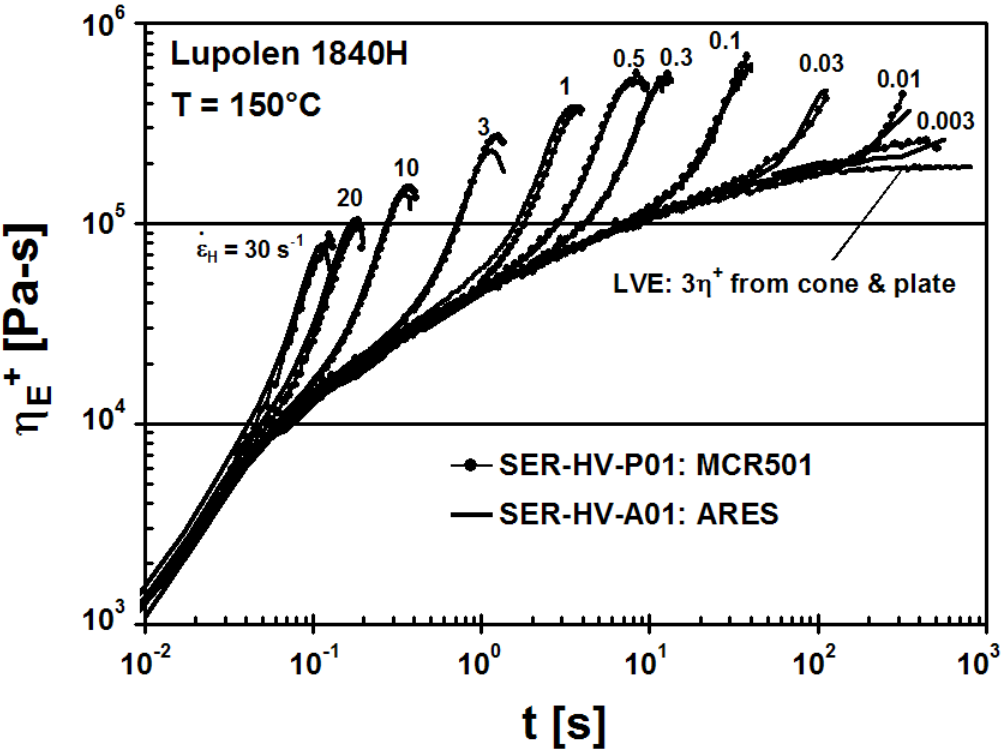

Figure 6: Tensile stress growth curves at a melt temperature of 150°C for Lupolen 1840H over a range of Hencky strain rates from 0.003 to 30 s^{-1} generated with the SER on two different host platforms, an MCR501 and an ARES, and a plot of LVE $3\eta^+$ shear stress growth data taken from cone and plate measurements in start-up of steady shear at a shear rate of 0.005 s^{-1}.

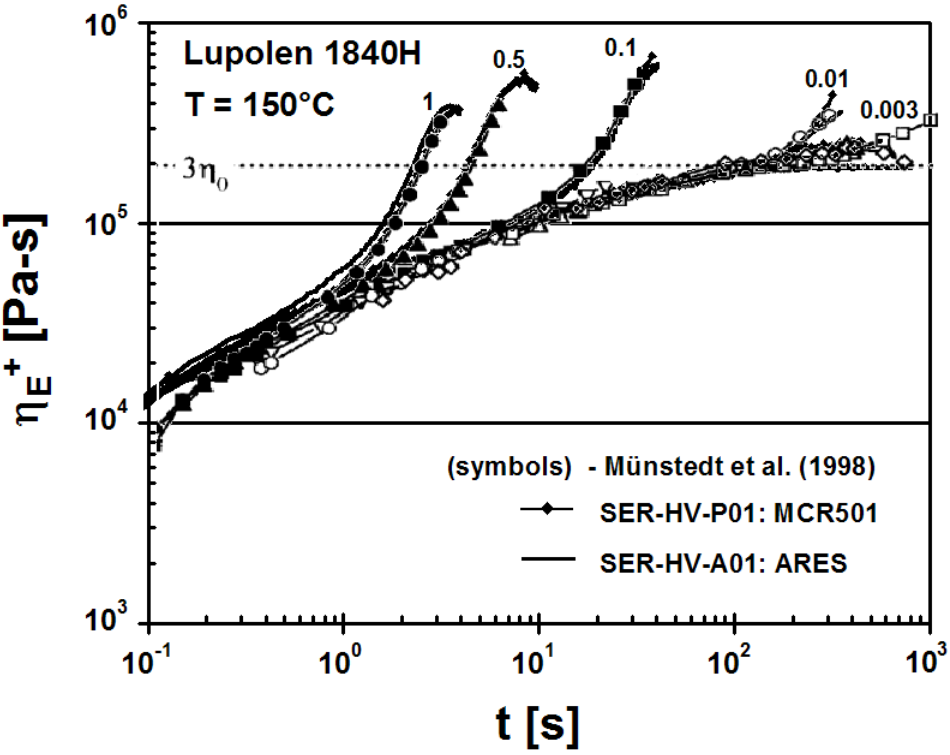

Figure 7: Comparison of tensile stress growth data at a melt temperature of 150°C for Lupolen 1840H over a range of Hencky strain rates from 0.003 to 1 s^{-1} generated with the SER on two different host platforms (solid lines) with extensional data taken from the literature (symbols with lines from Münstedt, 1998).

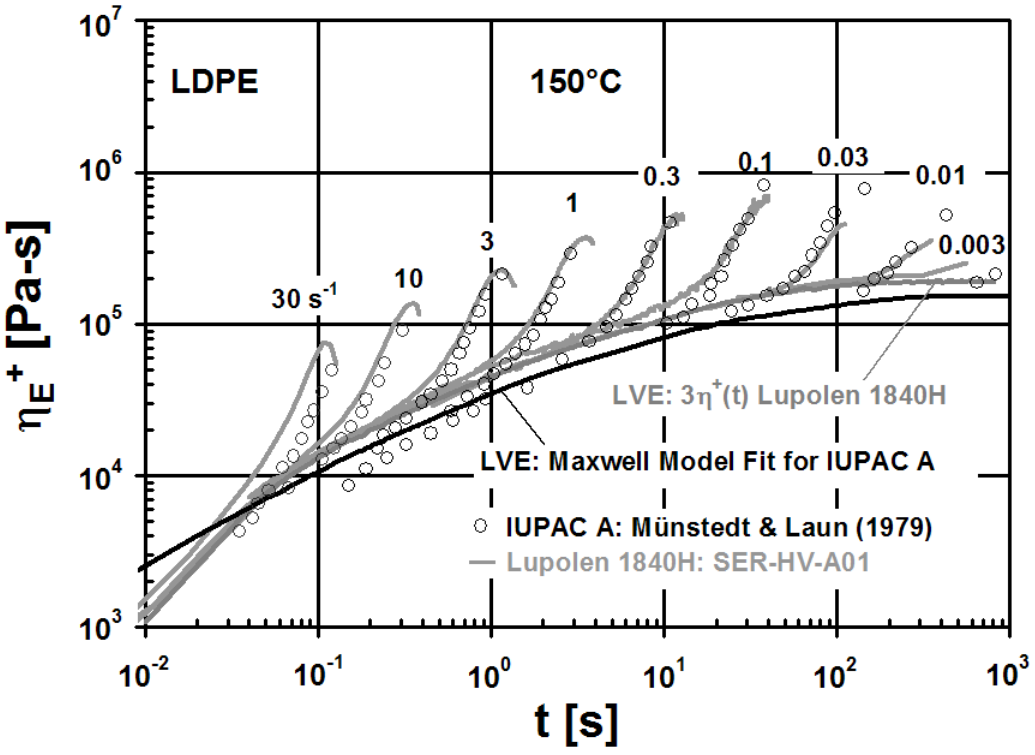

Figure 8: Comparison of tensile stress growth data at a melt temperature of 150°C over a range of Hencky strain rates from 0.003 to 30 s^{-1} for Lupolen 1840H generated with the SER (solid lines) and for IUPAC A taken from the literature (symbols from Münstedt & Laun, 1979).

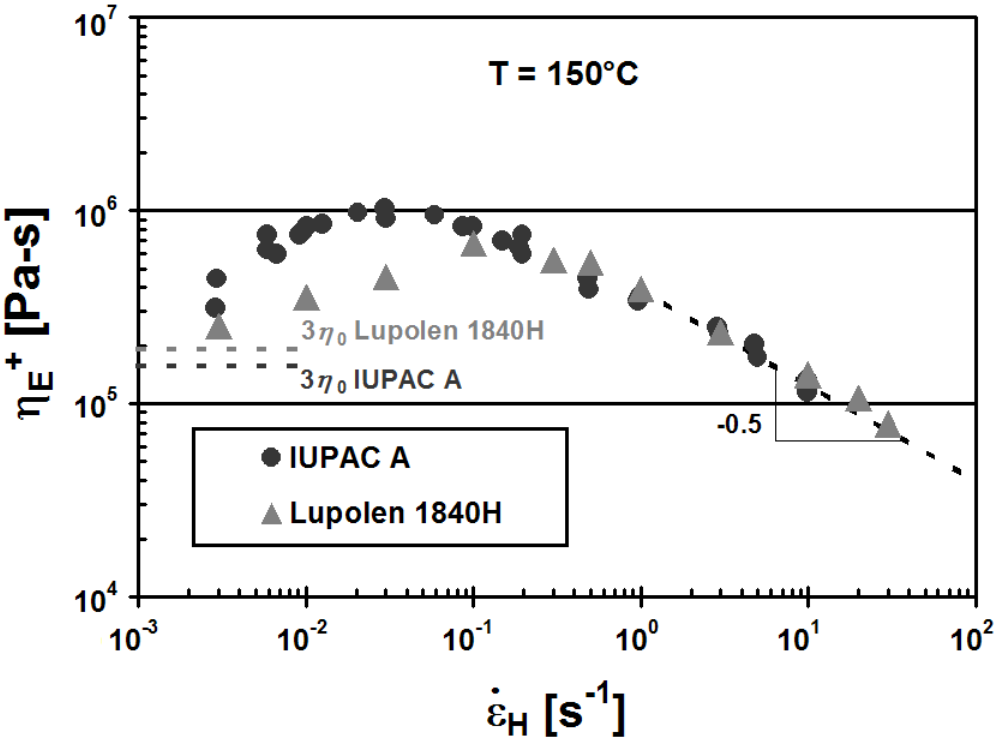

Figure 9: Comparison of the steady-state extensional viscosity behavior as a function of Hencky strain rate at a melt temperature of 150°C for Lupolen 1840H generated with the SER (triangles) and for IUPAC A taken from the literature (circles from Münstedt & Laun, 1979).

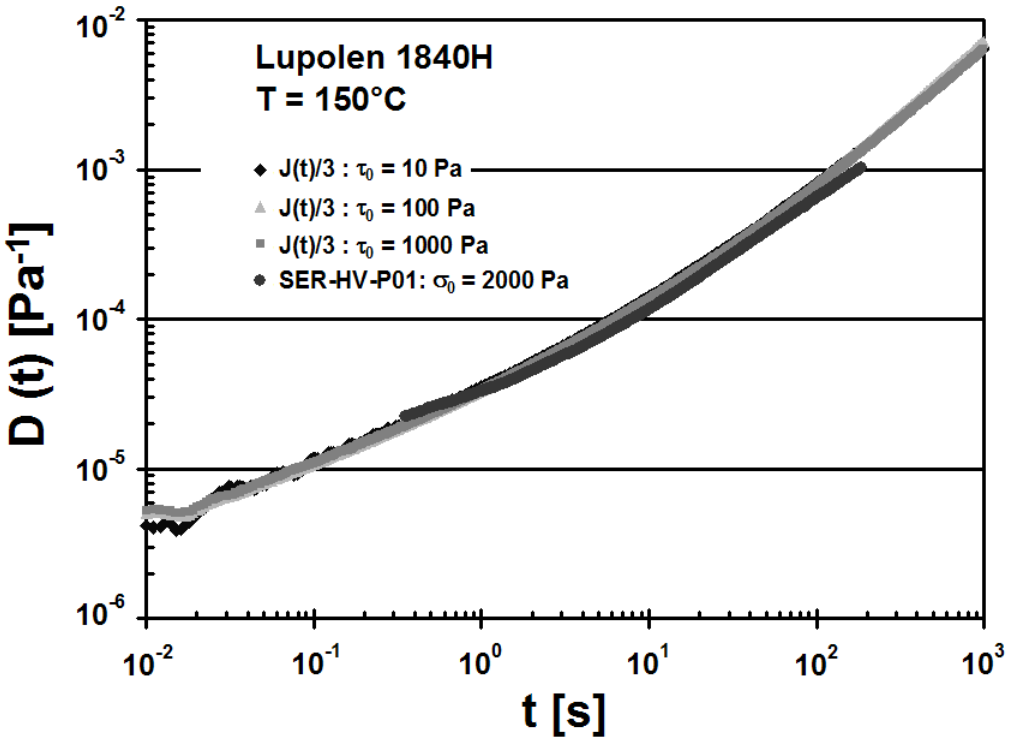

Figure 10: Comparison of shear creep compliance measurements for Lupolen 1840H from BASF at three stresses (150°C) with tensile creep compliance measurements generated with the SER on a MCR501 host platform.

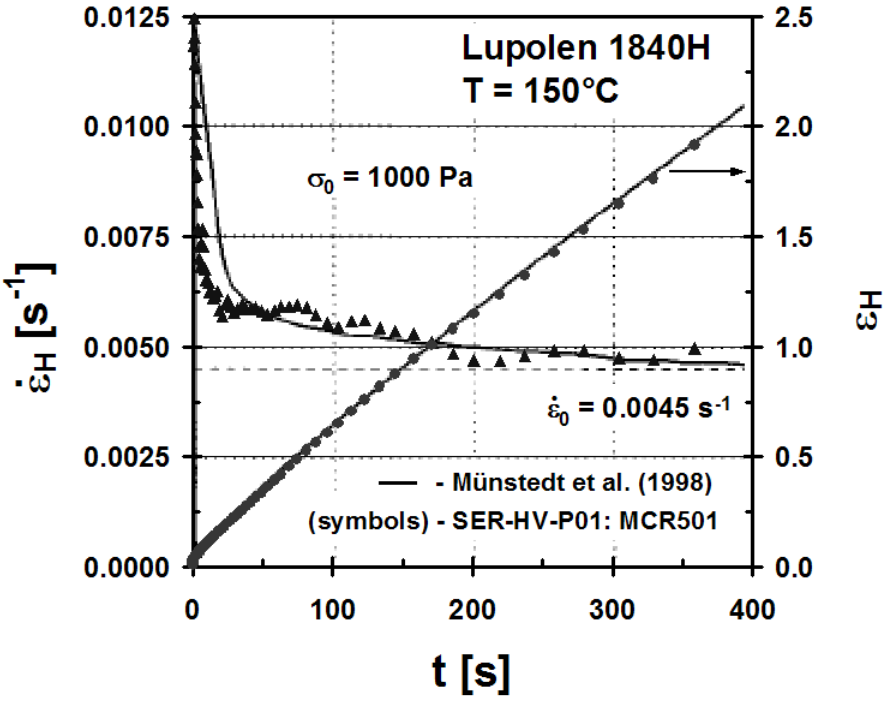

Figure 11: Comparison of tensile creep compliance data at a melt temperature of 150°C for Lupolen 1840H at a tensile creep stress of 1000 Pa generated with the SER (symbols) with tensile creep compliance data taken from the literature (solid lines from Münstedt, 1998).

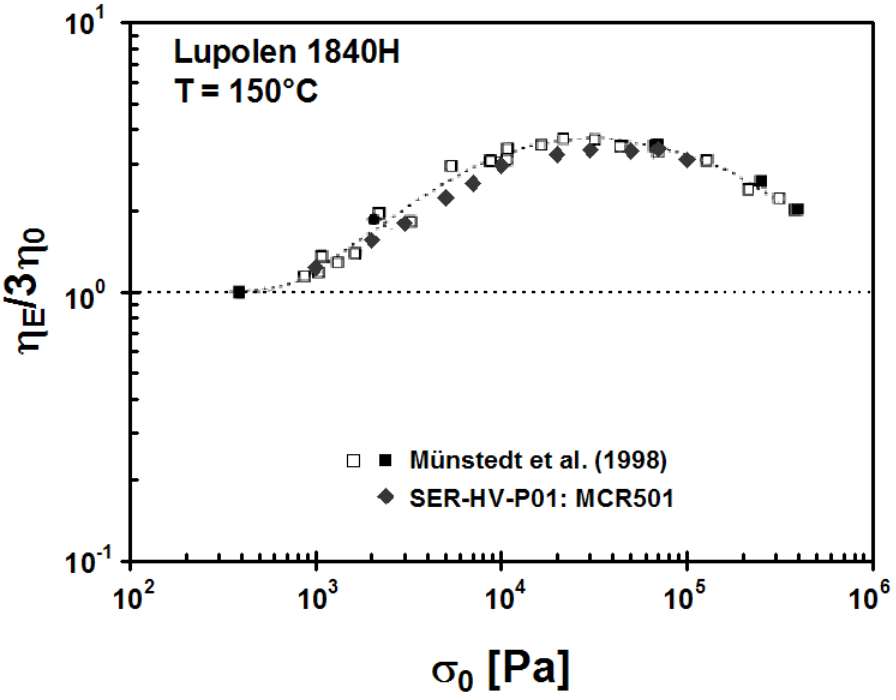

Figure 12: Comparison of steady-state extensional viscosity η_E (scaled with $3\eta_0$) as a function of the imposed tensile creep stress at a melt temperature of 150°C for Lupolen 1840H generated with the SER (diamond symbols) with data taken from the literature (square symbols from Münstedt, 1998).

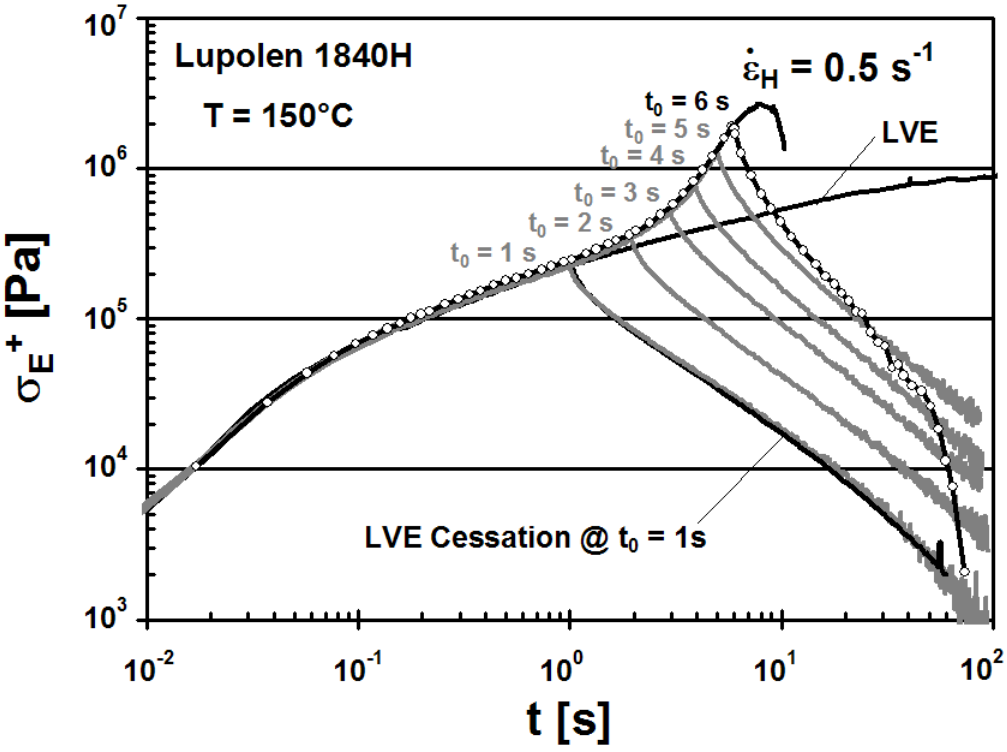

Figure 13: Cessation of steady extension rate experiments at a melt temperature of 150°C for Lupolen 1840H at a Hencky strain rate of 0.5 s^{-1} and cessation times, t_0, (from bottom to top) of 1, 2, 3, 4, 5, and 6 seconds.

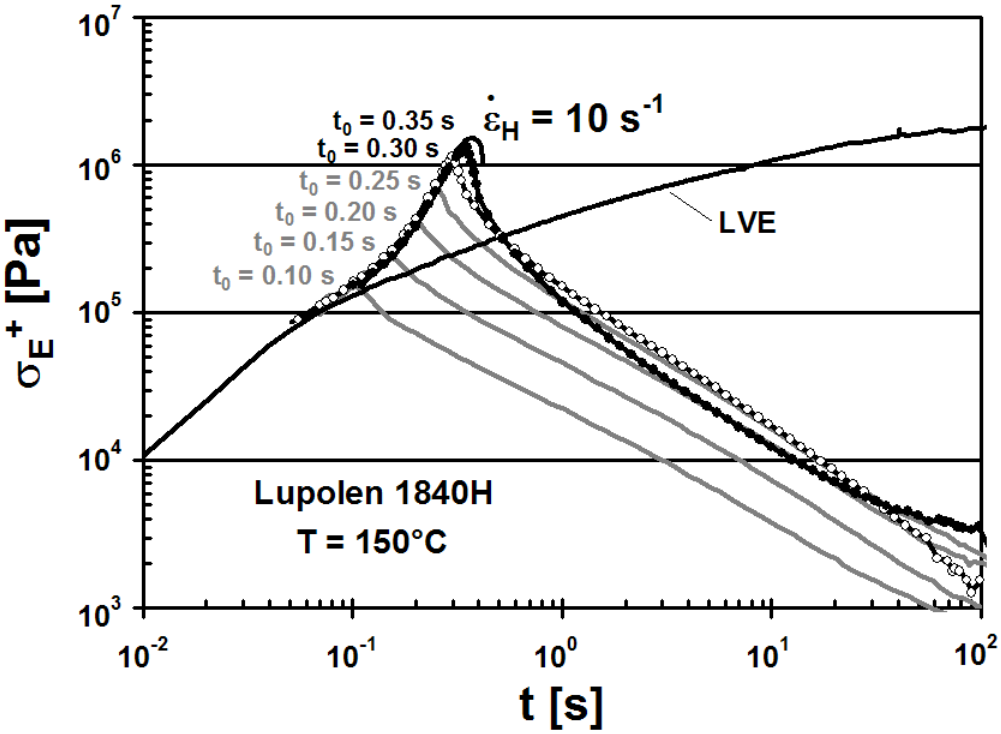

Figure 14: Cessation of steady extension rate experiments at a melt temperature of 150°C for Lupolen 1840H at a Hencky strain rate of 10 s^{-1} and cessation times, t_0, (from bottom to top) of 0.10, 0.15, 0.20, 0.25, 0.30, and 0.35 seconds.

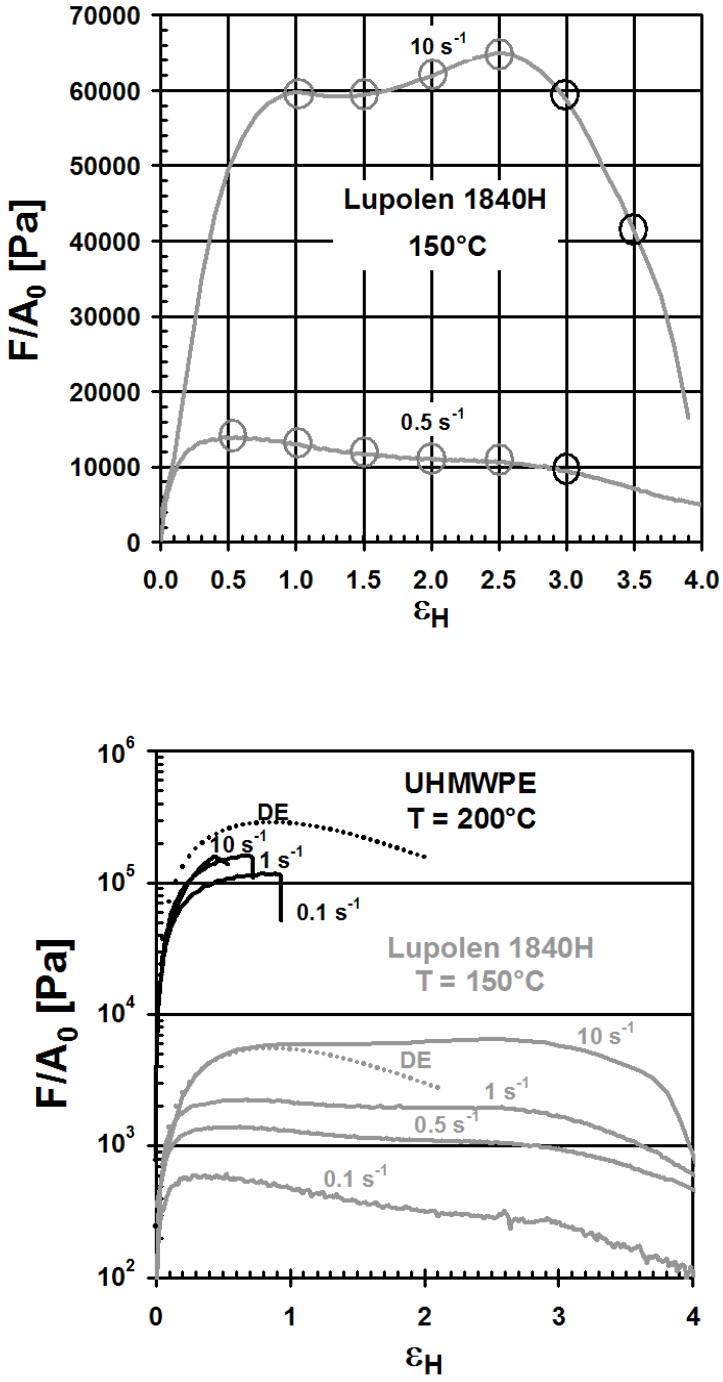

Figure 15: Evolution of the engineering tensile stress with Hencky strain over a range of Hencky strain rates: (a) data for Lupolen 1840H at a melt temperature of 150°C at Hencky strain rates of 0.5 and 10 s^{-1}. The large open circles indicate the Hencky strains at which the stress relaxation experiments were performed. (b) Comparison with data for UHMWPE at a melt temperature of 200°C. The broken lines show the predictions of the Doi-Edwards theory in the rapid stretching limit (see Eq. 9).

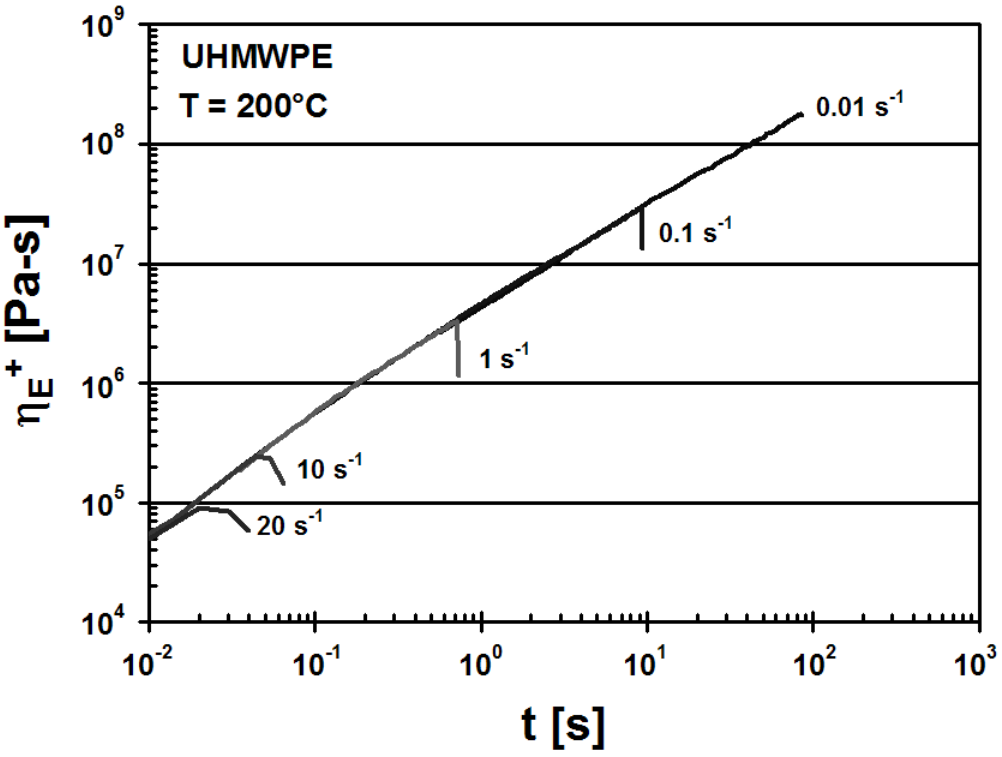

Figure 16. The transient extensional viscosity of an UHMWPE melt tested in the SER. The extensional viscosity continues to grow without bound at all extension rates until onset of necking instability and the sample ruptures.